

Three-Dimensional Graphene–TiO₂ Nanocomposite Photocatalyst Synthesized by Covalent Attachment

Jaehyeung Park,[†] Tong Jin,[‡] Chao Liu,[‡] Gonghu Li,[‡] and Mingdi Yan^{*,†,§}

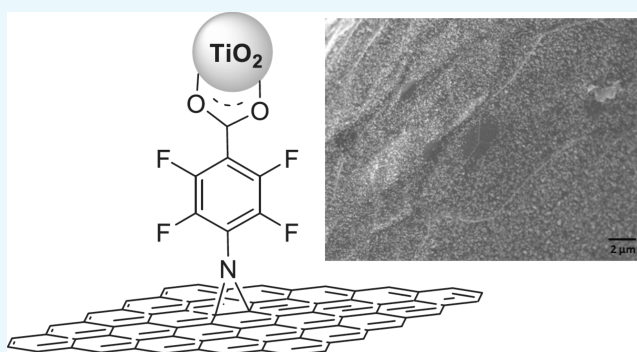
[†]Department of Chemistry, University of Massachusetts at Lowell, Lowell, Massachusetts 01854, United States

[‡]Department of Chemistry and Materials Science Program, University of New Hampshire, Durham, New Hampshire 03824, United States

[§]Department of Chemistry, KTH - Royal Institute of Technology, S-10044 Stockholm, Sweden

S Supporting Information

ABSTRACT: We report the synthesis of a three-dimensional graphene (3DG)–TiO₂ nanocomposite by covalently attaching P25 TiO₂ nanoparticles onto pristine 3DG through a perfluorophenyl azide-mediated coupling reaction. The TiO₂ nanoparticles were robustly attached on the 3DG surface, with minimal particle agglomeration. In photocatalytic CO₂ reduction, the 3DG–TiO₂ nanocomposite demonstrated excellent activity, about 11 times higher than that of the P25 TiO₂ nanoparticles. The enhanced activity can be partially attributed to the highly dispersed state of the P25 TiO₂ nanoparticles on the 3DG substrate. This 3DG-based system offers a new platform for fabricating photocatalytic materials with enhanced activities.



INTRODUCTION

Among the different forms of graphene, the recently developed three-dimensional graphene (3DG) has attracted increasing attention owing to its unique features.^{1,2} 3DG, with foamlike macrostructures, can be prepared by self-assembly,³ templating,⁴ or chemical vapor deposition (CVD).⁵ 3DG possesses many interesting properties in addition to those of typical two-dimensional graphene (2DG) nanosheets. For example, the interconnected porous structure of 3DG provides divergent pathways to conduct heat and electrons. The 3D nature of such materials eliminates intersheet contact resistance and reduces agglomeration of individual graphene nanosheets.^{1,2} Other desirable properties of 3DG include increased surface area, control over size and shape, and ease of handling and reuse. These features make 3DG a promising material for many applications, including photocatalysis and energy storage. Graphene has been shown to enhance the activities of semiconductor photocatalysts, where graphene acts as an electron acceptor and transporter in graphene–photocatalyst nanocomposite materials.^{6–13} The outstanding conductivity and electron mobility across the graphene network allow for rapid electron collection and transfer, suppressing electron–hole recombination, which lowers the photocatalytic activity of semiconductors. The relatively high specific surface areas of graphene materials also contribute to the enhanced photocatalytic efficiency of semiconductors. Recently, 3DG has been used to prepare nanocomposite materials with semiconductor photocatalysts¹⁴ by physisorption of TiO₂ nanoparticles onto 3D graphene oxide (3DGO)^{15,16} or 3DG^{17,18} or by

chemisorption onto 3DGO.¹⁹ Compared with physisorption, chemisorption provides a higher stability and stronger interactions between the individual components and subsequently improves the photocatalytic performance.^{11,12} For example, glucose was used as a linker between TiO₂ nanoparticles and 3DGO to achieve a higher stability and photocatalytic activity compared to those of the nanocomposite prepared without glucose.¹⁹ Although GO is relatively easier to prepare in large quantities, the oxidation process employed in its synthesis is usually detrimental to its electronic properties, which cannot be fully recovered even after subsequent reduction due to the presence of oxygen-containing species and defects introduced during the synthesis.²⁰

Here, we report a new 3DG–TiO₂ nanocomposite photocatalyst, synthesized by covalently attaching P25 TiO₂ nanoparticles onto pristine 3DG by perfluorophenyl azide (PFPA)-mediated coupling chemistry.^{21–23} We expect that the TiO₂ nanoparticles would be uniformly distributed on 3DG, with minimal particle agglomeration. Agglomeration is detrimental to the photocatalytic activity of TiO₂, as it reduces the surface area accessible to adsorb the reagents. In conjunction with pristine 3DG, the resulting nanocomposite material would have enhanced photocatalytic activities, for example, CO₂ reduction, compared to those of P25 TiO₂ alone.

Received: July 7, 2016

Accepted: August 16, 2016

Published: September 7, 2016

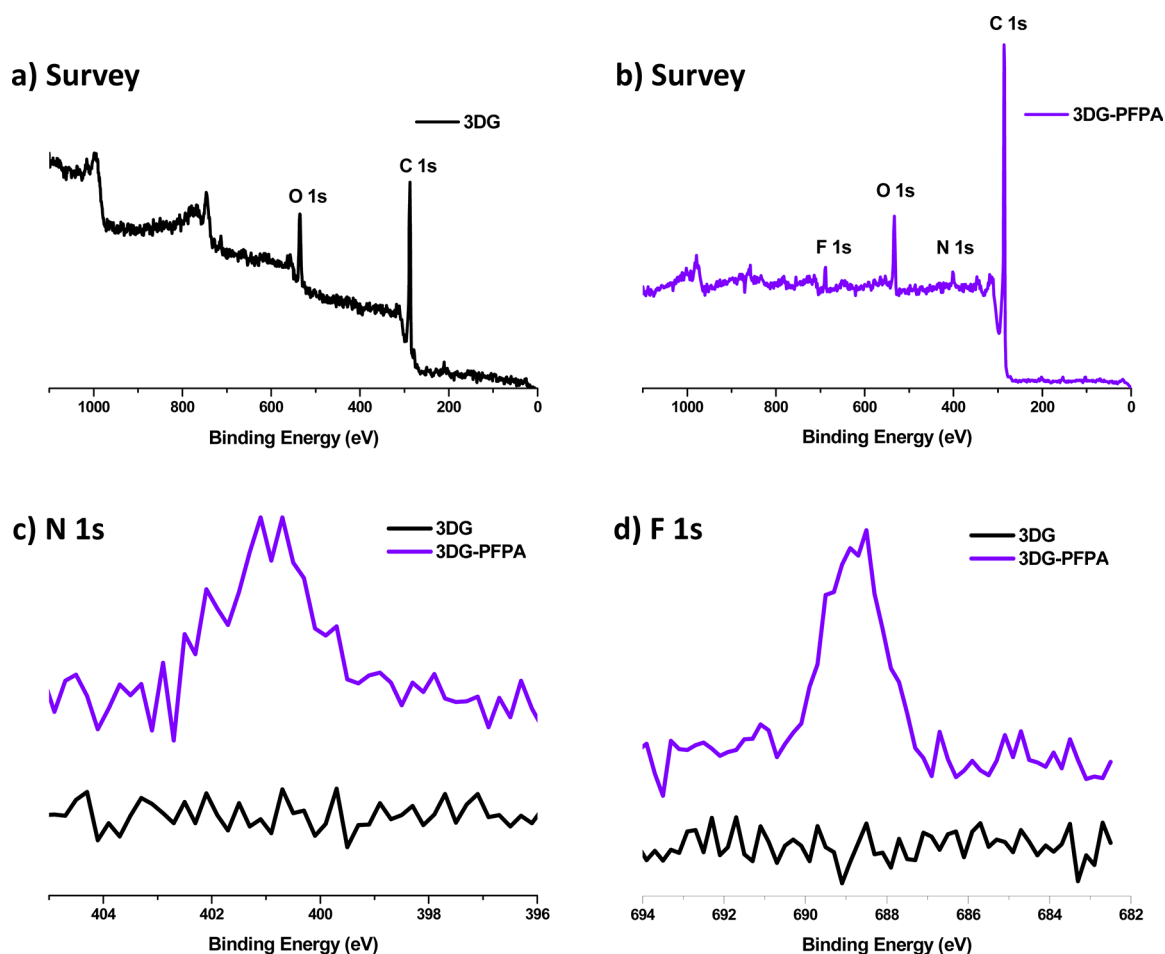
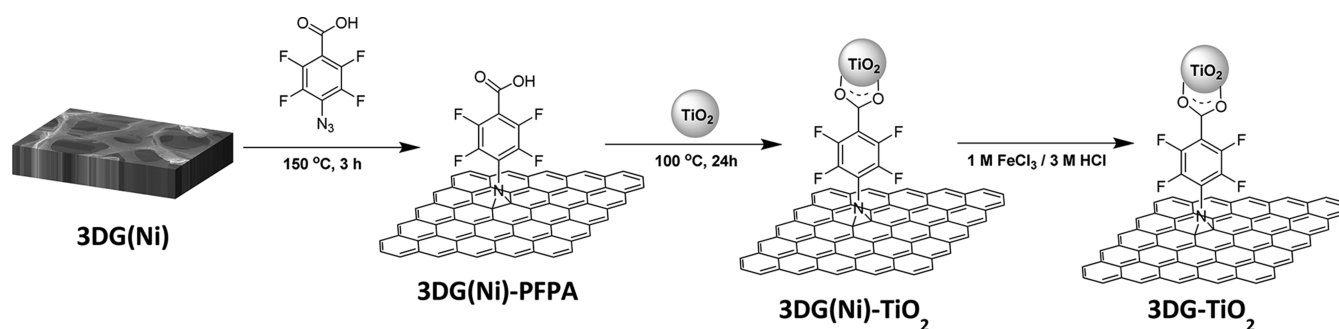
Scheme 1. Synthesis of 3DG–TiO₂

Figure 1. XPS survey spectra of 3DG (a) before and (b) after PFPA functionalization and corresponding high-resolution spectra: (c) N 1s and (d) F 1s. XPS spectra were referenced to the binding energy of adventitious carbon at 285.0 eV (C 1s).

EXPERIMENTAL SECTION

Materials. Methyl pentafluorobenzoate (>97%), sodium azide, AEROXIDE TiO₂ P25, acetone, ethyl ether, methanol, triethylamine (>99%), *N*-methyl-2-pyrrolidone (NMP), and hydrochloric acid (37%) were purchased from Sigma-Aldrich and were used as received, without any further purification. Nickel foam (Ni, 95% porosity, thickness 1.6 mm) was purchased from MTI Corp.

Preparation of 3DG and 2DG. 3DG on nickel (Ni) foam was prepared on the AIXTRON CVD equipment. Interconnected Ni foam was used as the substrate. The Ni foam was cut into small pieces (2 × 2 cm²). It was first annealed in an Ar/H₂ atmosphere at 1000 °C for 1 h to increase the grain size and

clean the surface. Graphene layers were then grown by introducing ultra-high-purity CH₄ gas for 30 min. After exposure to CH₄, the furnace was cooled to room temperature. The Raman spectrum of prepared Ni–G is shown in Figure S1.

2DG was prepared by liquid-phase exfoliation. Graphite flakes (Sigma) were dispersed in NMP to give a concentration of 1 mg/mL, and the mixture was sonicated using a sonication probe (20 kHz, 40% Ampl.; SONICS) for 24 h. The resulting dispersion was then centrifuged for 30 min at 500 rpm, and the supernatant was collected.

Preparation of 3DG–TiO₂ and 2DG–TiO₂. 4-Azido-2,3,5,6-tetrafluorobenzoic acid (PFPA-COOH) was synthesized following the previously reported protocol.^{24–26} A piece of 3DG(Ni) was placed in a solution of PFPA-COOH (88 mg) in

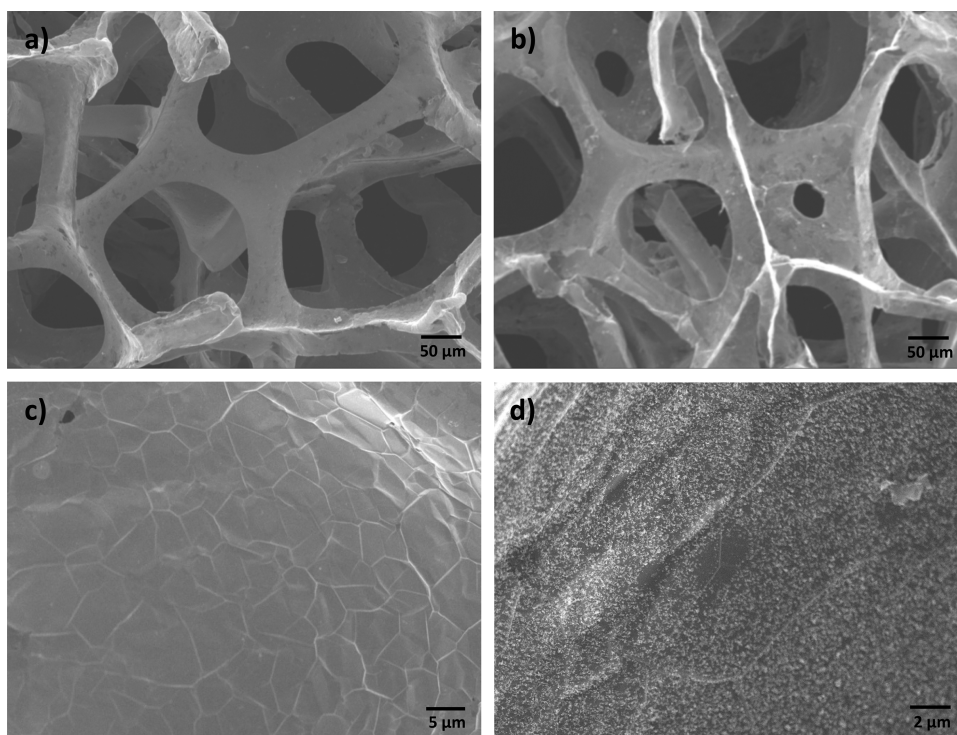


Figure 2. SEM images of (a,c) 3DG and (b,d) 3DG–TiO₂. Images (c) and (d) were taken at a higher magnification.

NMP (15 mL) and heated at 150 °C for 3 h. The sample was then washed with acetone to remove excess reagents. The PFPA-functionalized 3DG(Ni) and P25 TiO₂ nanoparticles (~5 mg) were dispersed in ethanol and heated at 100 °C in a Teflon-lined stainless steel autoclave for 24 h. The Ni foam support was then etched away by immersing the resulting sample in a solution of 1 M FeCl₃ and 3 M HCl. Free-standing 3DG–TiO₂ was obtained after rinsing the sample with HCl followed by water. The control sample, 2DG–TiO₂, was prepared following the same protocol as that for 3DG–TiO₂, by surface functionalization with PFPA-COOH and covalent attachment of P25 TiO₂ nanoparticles.

Characterization. Raman spectra were recorded on a SENTERRA Raman microscope (Bruker) system with a 532 nm wavelength laser. Infrared (IR) spectra were obtained with a Nicolet 6700 Fourier transform infrared spectrometer (Thermo Scientific). Scanning electron microscopy (SEM) images were acquired on a field-emission SEM (JSM 7401F; JEOL) equipped with an Oxford INCA energy dispersive X-ray spectroscopy (EDX) system. Transmission electron microscopy (TEM) images were obtained on a Philips EM400T microscope operated at 120 kV. X-ray powder diffraction (XRD) patterns were obtained on a Scintag PAD X X-ray diffractometer using Cu K α radiation. X-ray photoelectron spectroscopy (XPS) measurements were carried out on a Vacuum Generators Escalab MK II X-ray photoelectron spectrometer. All XPS spectra were referenced to the binding energy of the C 1s of adventitious carbon at 285.0 eV. Elemental analysis was conducted by acid digestion of solid samples, followed by quantification using a Varian Vista AX inductively coupled plasma atomic emission spectrometer. The optical absorption properties of the materials were obtained on a Cary 50 Bio spectrophotometer. A Barreliano diffuse reflectance probe was used to collect UV–visible spectra, using BaSO₄ as a standard.

Photocatalytic CO₂ Reduction. Before photocatalysis, a piece of 3DG–TiO₂ (dimension 2 × 2 × 0.1 cm³) or 1 mg of P25 TiO₂ was placed in a sealed test tube. The test tube was purged with a mixture of high-purity CO₂ gas (99.999%, Airgas) and triethylamine vapor for 20 min. The sample was then irradiated with a 200 W mercury lamp. The light intensity on the sample was fixed at 140 mW/cm². The head space was sampled with a gas-tight syringe at different time intervals for product analysis using Agilent 7820 GC, equipped with a thermal conductivity detector and a 60/80 Carboxen-1000 packed column (Supelco).

RESULTS AND DISCUSSION

3DG was prepared by growing graphene on an interconnected nickel (Ni) foam by CVD at 1000 °C using CH₄ gas as the precursor.⁵ The Raman spectrum of the synthesized sample, 3DG(Ni), shows the presence of both single- and multi-layered graphene (Figure S1). This is in good agreement with the typical 3DG samples grown on Ni foam by CVD, which is attributed to the polycrystalline nature of nickel foam.⁵ Further analysis by XRD also confirms the graphene structure (Figure S2).

The 3DG–TiO₂ nanocomposite photocatalyst was synthesized using a straightforward procedure involving PFPA-mediated coupling chemistry, as shown in Scheme 1 (see Supporting Information for experimental details). In a typical synthesis, 3DG(Ni) was first functionalized with PFPA-COOH at 150 °C.^{27,28} The reaction occurred through the highly reactive perfluorophenyl nitrene intermediate, which gave the covalent adduct and introduced carboxyl groups on 3DG.^{21–23,29–33} The covalent functionalization of graphene was followed by XPS. Before the XPS analysis, the Ni foam support was etched away in a solution of FeCl₃/HCl. The PFPA-functionalized 3DG showed F 1s (689 eV) and N 1s (401 eV) peaks (Figure 1b), which were absent in the spectrum

of 3DG (Figure 1a). Furthermore, the N 1s peaks of the azide, at 402.1 and 405.6 eV, with an intensity ratio of 2:1,³² were not seen in the spectrum of PFPA-functionalized 3DG. Instead, only one peak at 401 eV was observed (Figure 1c), which could be assigned to the N in the PFPA-functionalized graphene structure.³³ The presence of the F 1s peak at 689 eV after functionalization of 3DG with PFPA (Figure 1d) is consistent with our previous results for PFPA-functionalized graphene.^{32,33} Taken together, these results provided clear evidence for the successful functionalization of 3DG with PFPA.

The commercially available TiO₂ nanoparticles, Degussa P25, were used to synthesize the nanocomposite photocatalyst. The TiO₂ nanoparticles were covalently attached onto 3DG(Ni)-PFPA through binding with the carboxyl groups on the 3DG surface (Scheme 1) by a solvothermal process.³⁴ This was done before removing the Ni foam substrate to maintain the 3DG(Ni)-PFPA framework during the solvothermal treatment to attach the TiO₂ nanoparticles.³⁴ After washing the resulting material with ethanol to remove excess P25 nanoparticles, the Ni foam substrate was etched away using FeCl₃/HCl. Free-standing 3DG-TiO₂ was obtained after rinsing the synthesized nanocomposite with HCl and water.

The morphology of 3DG and 3DG-TiO₂ was examined using SEM. The interconnected 3DG structure with a pore size of ~200 μm was well maintained without collapsing or cracking during the etching of the Ni foam substrate by the acid (Figure 2a,b). The ripples and wrinkles observed on the graphene surface (Figure 2c,d) are common for graphene fabricated on a Ni substrate, which are induced by the difference in the thermal expansion coefficients of graphene and Ni.³⁵ After the attachment of TiO₂ nanoparticles, highly dispersed nanoparticles ~20 nm in size were observed on 3DG (Figure 2d). The TiO₂ nanoparticles were evenly distributed on the 3DG surface, without significant agglomeration. Furthermore, these results demonstrate that the PFPA covalent coupling chemistry was robust, and the TiO₂ nanoparticles remained firmly attached on the 3DG surface even after the samples were subjected to strong acid treatment.

Control experiments were carried out to further confirm the covalent attachment of TiO₂ nanoparticles on 3DG. In one experiment, samples were prepared from 3DG in the same manner except that the 3DG was not functionalized with PFPA-COOH. In this case, only a few aggregates of TiO₂ nanoparticles were seen on the 3DG surface (Figure S3), suggesting that the TiO₂ nanoparticles were conjugated on 3DG through the PFPA coupling chemistry in the 3DG-TiO₂ nanocomposite. In another control experiment, 2DG flakes, prepared by exfoliating the graphite powder in NMP under sonication, were functionalized with PFPA-COOH, followed by covalent attachment of P25 TiO₂ nanoparticles. In the resulting material (2DG-TiO₂), most of the TiO₂ nanoparticles were agglomerated (Figure S4), suggesting that the framework of 3DG is important in dispersing the TiO₂ nanoparticles. In addition, the TiO₂ nanoparticles on the 3DG-TiO₂ nanocomposite prepared by PFPA coupling chemistry showed a higher dispersibility than that on 2DG-TiO₂³⁶ or 3DG-TiO₂ materials prepared by other methods.^{16,18}

Furthermore, the 3DG-TiO₂ nanocomposite was characterized by XRD. Figure 3 shows the XRD pattern of 3DG-TiO₂. The typical diffraction peaks of P25 TiO₂, consisting of both the anatase phase [$2\theta = 25^\circ$ (101), 37° (004), 38° (112), 48° (200)] and the rutile phase [$2\theta = 27^\circ$ (110), 36° (101),

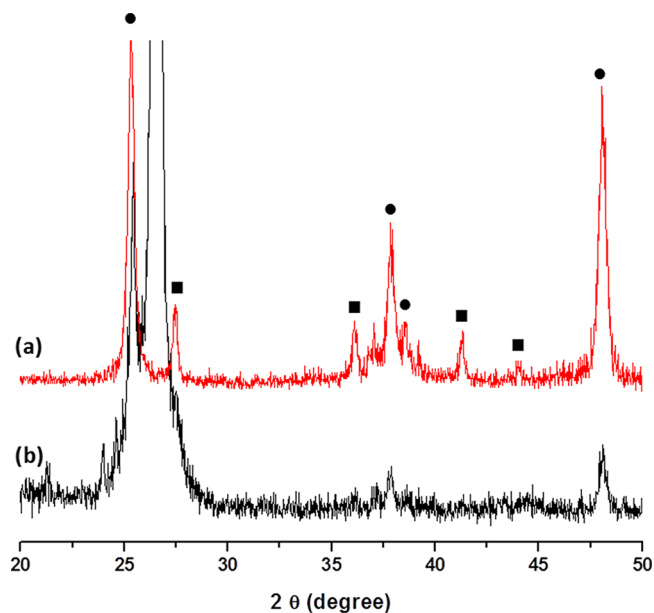


Figure 3. XRD patterns of (a) P25 TiO₂ and (b) 3DG-TiO₂ (●: anatase, ■: rutile).

41° (111), 44° (210)], were observed.³⁶ The intense diffraction peak at $2\theta = 26.5^\circ$ is characteristic of the (002) hexagonal graphitic carbon (JCPDS card No. 75-1621) in 3DG (Figures 3 and S2).³⁷ The presence of Ti and O in 3DG-TiO₂ was also confirmed by EDX (Figure S5). The Ti content was determined to be 2.9 mmol/g on 3DG-TiO₂ by elemental analysis after acid digestion of the nanocomposite material.

3DG-TiO₂ was tested for its performance in photocatalytic CO₂ reduction in comparison to that of P25 TiO₂, using triethylamine as a sacrificial electron donor (Figure 4). Under the experimental conditions employed in this study, CO was observed to be the only gaseous product upon photocatalytic CO₂ reduction. After 4 h, the amounts of CO generated per per milligram of TiO₂ were 0.11 and 1.26 μmol/mg for P25 TiO₂ and 3DG-TiO₂, respectively. This represents an 11-fold higher activity for 3DG-TiO₂ than that for P25 TiO₂. This

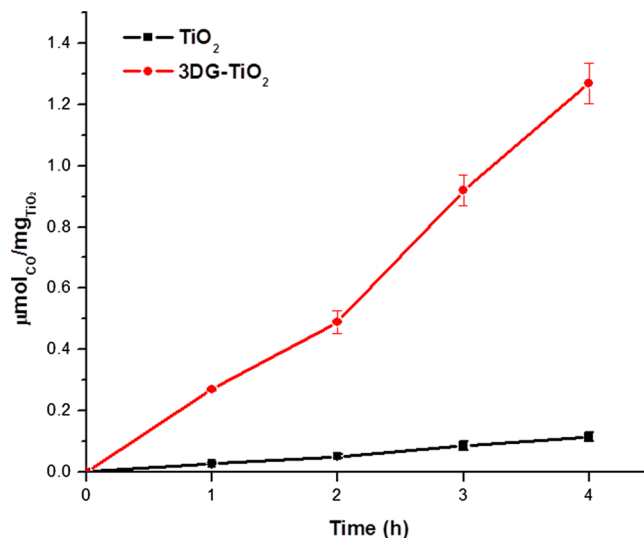


Figure 4. Production of CO on photocatalytic CO₂ reduction at the gas-surface interface. No solvent was used in photocatalytic testing.

enhancement in photocatalytic activity can be attributed to the high specific surface area of the 3DG support and the excellent dispersion of TiO₂ nanoparticles on 3DG in the 3DG–TiO₂ nanocomposite, which provide more accessible surfaces to reagents and better light harvesting. Other contributing factors include the strong interactions between the TiO₂ nanoparticles and 3DG, resulting from the covalent attachment. Further studies using electrochemical methods are underway to probe possible electronic interactions between TiO₂ nanoparticles and the 3DG framework.

CONCLUSION

In summary, we synthesized a new graphene-based photocatalyst consisting of TiO₂ nanoparticles covalently attached to 3DG. The TiO₂ nanoparticles were well dispersed on the 3DG surface, without significant agglomeration. This nanocomposite material demonstrated a considerably higher activity than that of bare TiO₂ in photocatalytic CO₂ reduction, likely due to the high specific surface area of the 3DG substrate, the strong interactions, and the excellent dispersion of TiO₂ nanoparticles on 3DG. The new 3DG–TiO₂ nanocomposite materials could find other potential applications, including energy storage and environmental decontamination.

ASSOCIATED CONTENT

Supporting Information

The Supporting Information is available free of charge on the ACS Publications website at DOI: 10.1021/acsomega.6b00113.

Raman spectra, optical image, and X-ray powder diffractogram of 3DG; EDX spectra of 3DG and 3DG–TiO₂; SEM image of the control sample; TEM image of 2DG–TiO₂; UV–visible diffuse reflectance spectra of TiO₂, 3DG, and 3DG–TiO₂ (PDF)

AUTHOR INFORMATION

Corresponding Author

*E-mail: Mingdi_Yan@uml.edu (M.Y.).

Notes

The authors declare no competing financial interest.

ACKNOWLEDGMENTS

This work was supported by the National Science Foundation (CHE-1112436 to M.Y. and CBET-1510810 to G.L.). We thank Michael Louis, Jake Riffle, Dr. Shawna Hollen, and Thomas Fenton for helpful discussions.

REFERENCES

- (1) Patil, U.; Lee, S. C.; Kulkarni, S.; Sohn, J. S.; Nam, M. S.; Han, S.; Jun, S. C. Nanostructured pseudocapacitive materials decorated 3D graphene foam electrodes for next generation supercapacitors. *Nanoscale* **2015**, *7*, 6999–7021.
- (2) Nardocchia, S.; Carriazo, D.; Ferrer, M. L.; Gutierrez, M. C.; del Monte, F. Three dimensional macroporous architectures and aerogels built of carbon nanotubes and/or graphene: synthesis and applications. *Chem. Soc. Rev.* **2013**, *42*, 794–830.
- (3) Xu, Y.; Sheng, K.; Li, C.; Shi, G. Self-Assembled Graphene Hydrogel via a One-Step Hydrothermal Process. *ACS Nano* **2010**, *4*, 4324–4330.
- (4) Choi, B. G.; Yang, M.; Hong, W. H.; Choi, J. W.; Huh, Y. S. 3D Macroporous Graphene Frameworks for Supercapacitors with High Energy and Power Densities. *ACS Nano* **2012**, *6*, 4020–4028.
- (5) Chen, Z.; Ren, W.; Gao, L.; Liu, B.; Pei, S.; Cheng, H.-M. Three-dimensional flexible and conductive interconnected graphene net-

works grown by chemical vapour deposition. *Nat. Mater.* **2011**, *10*, 424–428.

- (6) Zhang, Y.; Tang, Z.-R.; Fu, X.; Xu, Y.-J. TiO₂–Graphene Nanocomposites for Gas-Phase Photocatalytic Degradation of Volatile Aromatic Pollutant: Is TiO₂–Graphene Truly Different from Other TiO₂–Carbon Composite Materials? *ACS Nano* **2010**, *4*, 7303–7314.

- (7) Zhang, N.; Zhang, Y.; Xu, Y.-J. Recent progress on graphene-based photocatalysts: current status and future perspectives. *Nanoscale* **2012**, *4*, 5792–5813.

- (8) Xiang, Q.; Yu, J.; Jaroniec, M. Graphene-based semiconductor photocatalysts. *Chem. Soc. Rev.* **2012**, *41*, 782–796.

- (9) Upadhyay, R. K.; Sooin, N.; Roy, S. S. Role of graphene/metal oxide composites as photocatalysts, adsorbents and disinfectants in water treatment: a review. *RSC Adv.* **2014**, *4*, 3823–3851.

- (10) Yang, M.-Q.; Zhang, N.; Pagliaro, M.; Xu, Y.-J. Artificial photosynthesis over graphene-semiconductor composites. Are we getting better? *Chem. Soc. Rev.* **2014**, *43*, 8240–8254.

- (11) Xiang, Q.; Cheng, B.; Yu, J. Graphene-Based Photocatalysts for Solar-Fuel Generation. *Angew. Chem., Int. Ed.* **2015**, *54*, 11350–11366.

- (12) Zhang, N.; Yang, M.-Q.; Liu, S.; Sun, Y.; Xu, Y.-J. Waltzing with the Versatile Platform of Graphene to Synthesize Composite Photocatalysts. *Chem. Rev.* **2015**, *115*, 10307–10377.

- (13) Yang, M.-Q.; Xu, Y.-J. Photocatalytic conversion of CO₂ over graphene-based composites: current status and future perspective. *Nanoscale Horiz.* **2016**, *1*, 185–200.

- (14) Park, J.; Yan, M. Three-dimensional graphene-TiO₂ hybrid nanomaterial for high efficient photocatalysis. *Nanotechnol. Rev.* **2016**, *5*, 417–423.

- (15) Kim, H.-N.; Yoo, H.; Moon, J. H. Graphene-embedded 3D TiO₂ inverse opal electrodes for highly efficient dye-sensitized solar cells: morphological characteristics and photocurrent enhancement. *Nanoscale* **2013**, *5*, 4200–4204.

- (16) Zhang, Z.; Xiao, F.; Guo, Y.; Wang, S.; Liu, Y. One-Pot Self-Assembled Three-Dimensional TiO₂–Graphene Hydrogel with Improved Adsorption Capacities and Photocatalytic and Electrochemical Activities. *ACS Appl. Mater. Interfaces* **2013**, *5*, 2227–2233.

- (17) Lee, D. H.; Song, D.; Kang, Y. S.; Park, W. I. Three-Dimensional Monolayer Graphene and TiO₂ Hybrid Architectures for High-Efficiency Electrochemical Photovoltaic Cells. *J. Phys. Chem. C* **2015**, *119*, 6880–6885.

- (18) Zhi, J.; Cui, H.; Chen, A.; Xie, Y.; Huang, F. Efficient highly flexible dye sensitized solar cells of three dimensional graphene decorated titanium dioxide nanoparticles on plastic substrate. *J. Power Sources* **2015**, *281*, 404–410.

- (19) Qiu, B.; Xing, M.; Zhang, J. Mesoporous TiO₂ Nanocrystals Grown in Situ on Graphene Aerogels for High Photocatalysis and Lithium-Ion Batteries. *J. Am. Chem. Soc.* **2014**, *136*, 5852–5855.

- (20) Loh, K. P.; Bao, Q.; Eda, G.; Chhowalla, M. Graphene oxide as a chemically tunable platform for optical applications. *Nat. Chem.* **2010**, *2*, 1015–1024.

- (21) Liu, L.-H.; Yan, M. Simple Method for the Covalent Immobilization of Graphene. *Nano Lett.* **2009**, *9*, 3375–3378.

- (22) Liu, L.-H.; Lerner, M. M.; Yan, M. Derivatization of pristine graphene with well-defined chemical functionalities. *Nano Lett.* **2010**, *10*, 3754–3756.

- (23) Park, J.; Yan, M. Covalent functionalization of graphene with reactive intermediates. *Acc. Chem. Res.* **2013**, *46*, 181–189.

- (24) Liu, L.; Yan, M. A general approach to the covalent immobilization of single polymers. *Angew. Chem., Int. Ed.* **2006**, *45*, 6207–6210.

- (25) Wang, H.; Ren, J.; Hlaing, A.; Yan, M. Fabrication and anti-fouling properties of photochemically and thermally immobilized poly(ethylene oxide) and low molecular weight poly(ethylene glycol) thin films. *J. Colloid Interface Sci.* **2011**, *354*, 160–167.

- (26) Kubo, T.; Wang, X.; Tong, Q.; Yan, M. Polymer-Based Photocoupling Agent for Efficient Immobilization of Nanomaterials and Small Molecules. *Langmuir* **2011**, *27*, 9372–9378.

- (27) Wang, H.; Li, L.; Tong, Q.; Yan, M. Evaluation of photochemically immobilized poly(2-ethyl-2-oxazoline) thin films as

protein-resistant surfaces. *ACS Appl. Mater. Interfaces* **2011**, *3*, 3463–3471.

(28) Wang, H.; Zhang, Y.; Yuan, X.; Chen, Y.; Yan, M. A Universal Protocol for Photochemical Covalent Immobilization of Intact Carbohydrates for the Preparation of Carbohydrate Microarrays. *Bioconjugate Chem.* **2011**, *22*, 26–32.

(29) Liu, L.-H.; Zorn, G.; Castner, D. G.; Solanki, R.; Lerner, M. M.; Yan, M. A simple and scalable route to wafer-size patterned graphene. *J. Mater. Chem.* **2010**, *20*, 5041–5046.

(30) Liu, L.-H.; Yan, M. Perfluorophenyl Azides: New Applications in Surface Functionalization and Nanomaterial Synthesis. *Acc. Chem. Res.* **2010**, *43*, 1434–1443.

(31) Liu, L.-H.; Yan, M. Functionalization of pristine graphene with perfluorophenyl azides. *J. Mater. Chem.* **2011**, *21*, 3273–3276.

(32) Zorn, G.; Liu, L.-H.; Árnadóttir, L.; Wang, H.; Gamble, L. J.; Castner, D. G.; Yan, M. X-ray Photoelectron Spectroscopy Investigation of the Nitrogen Species in Photoactive Perfluorophenylazide-Modified Surfaces. *J. Phys. Chem. C* **2014**, *118*, 376–383.

(33) Park, J.; Jayawardena, H. S. N.; Chen, X.; Jayawardana, K. W.; Sundhoro, M.; Ada, E.; Yan, M. A General Method for the Fabrication of Graphene-Nanoparticle Hybrid Material. *Chem. Commun.* **2015**, *51*, 2882–2885.

(34) Qu, Q.; Geng, H.; Peng, R.; Cui, Q.; Gu, X.; Li, F.; Wang, M. Chemically Binding Carboxylic Acids onto TiO₂ Nanoparticles with Adjustable Coverage by Solvothermal Strategy. *Langmuir* **2010**, *26*, 9539–9546.

(35) Chae, S. J.; Güneş, F.; Kim, K. K.; Kim, E. S.; Han, G. H.; Kim, S. M.; Shin, H.-J.; Yoon, S.-M.; Choi, J.-Y.; Park, M. H.; Yang, C. W.; Pribat, D.; Lee, Y. H. Synthesis of Large-Area Graphene Layers on Poly-Nickel Substrate by Chemical Vapor Deposition: Wrinkle Formation. *Adv. Mater.* **2009**, *21*, 2328–2333.

(36) Zhang, H.; Lv, X.; Li, Y.; Wang, Y.; Li, J. P25-Graphene Composite as a High Performance Photocatalyst. *ACS Nano* **2010**, *4*, 380–386.

(37) Kulkarni, S. B.; Patil, U. M.; Shackery, I.; Sohn, J. S.; Lee, S.; Park, B.; Jun, S. High-performance supercapacitor electrode based on a polyaniline nanofibers/3D graphene framework as an efficient charge transporter. *J. Mater. Chem. A* **2014**, *2*, 4989–4998.